Acoustic Emission Monitoring of the Syracuse Athena Temple: Scale Invariance in the Timing of Ruptures

Acoustic Emission Monitoring of the Syracuse Athena Temple: Scale Invariance in the Timing of Ruptures

G. Niccolini
Istituto Nazionale di Ricerca Metrologica, Strada delle Cacce 91, 10135 Torino, Italy

A. Carpinteri, G. Lacidogna, and A. Manuello
Department of Structural Engineering, Politecnico di Torino, Corso Duca degli Abruzzi 24, 10129 Torino, Italy

We perform a comparative statistical analysis between the acoustic-emission time series from the ancient Greek Athena temple in Syracuse and the sequence of nearby earthquakes. We find an apparent association between acoustic-emission bursts and the earthquake occurrence. The waiting-time distributions for acoustic-emission and earthquake time series are described by a unique scaling law indicating self-similarity over a wide range of magnitude scales. This evidence suggests a correlation between the aging process of the temple and the local seismic activity.

Introduction.—Fracture in heterogeneous materials occurs as the culmination of progressive damage due to loading conditions or harsh environments. Damage growth is accompanied by the spontaneous release of stored strain energy in the form of transient elastic waves [acoustic emission (AE)] [1–3]. Thus, as it provides information on the internal state of a material, AE monitoring is used successfully for the structural integrity assessment of materials and also large-sized structures (buildings, bridges, etc.) before they become safety hazards [3,4]. This predictive power can be exploited to protect the Italian cultural heritage, as historic buildings and monuments are exposed to seismic risk. Many structures may undergo accelerated aging and deterioration due to the action of small and intermediate earthquakes, rather frequent in Southern Italy. The triggered damage, often inaccessible for visual inspection, eventually results in increased vulnerability to strong earthquakes. Here, the results of AE monitoring of the Athena temple in Syracuse (Eastern Sicily) are presented. We analyze the time correlation between the AE bursts from a temple pillar and the occurrence of nearby earthquakes. Furthermore, we investigate consistency of scaling laws between AE and Eastern Sicily earthquake waiting-time distributions.

AE Monitoring of the Syracuse Cathedral.—In the seventh century, the Cathedral of Syracuse (on the UNESCO World Heritage List since 2005) was built onto the ruins of the ancient and famed Athena temple and afterward repeatedly modified as a consequence of damages caused by earthquakes. The structure currently exhibits an extended damage pattern, especially in four pillars at the end of the nave, showing repaired areas, replacements, and also several cracks. The AE activity in one of the nave pillars was monitored over a four-month period by means of six piezoelectric transducers working in the range of 50–500 kHz attached to the pillar surface.

After setting an appropriate detection threshold to filter out environmental background noise, we started data acquisition storing two quantities for each AE signal: the arrival time, determined by using the first threshold crossing of the signal, and the peak amplitude $V_{\max}$ (expressed in μV), which defines the magnitude of the AE event as $M = \log(V_{\max}/1\ \mu\mathrm{V})$ [3].

Figure 1 displays the accumulated number of AE events, the AE instantaneous rate (averaged over 1 h), and the earthquake sequence as functions of time. Here, only earthquakes with hypocentral distance ≤ 60 km from Syracuse are considered (Fig. 2 and Table I). There appears to be a correlation in time between AE activity on the Cathedral and local seismicity, as AE bursts often follow the occurrence of nearby seismic events.

There appear to be some seismic events which follow AE bursts and, then, which do not trigger AE activity on the Cathedral. The occurrence of increased AE activity in several case histories from Italy was observed by Carpinteri, Lacidogna, and Niccolini and Gregori *et al.*

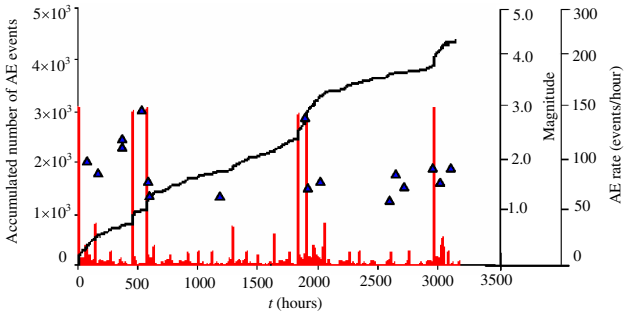

FIG. 1 (color online). Accumulated number (black line), instantaneous AE rate averaged over 1 h (red line) in the temple pillar, and nearby earthquake occurrence (triangles) as functions of time.

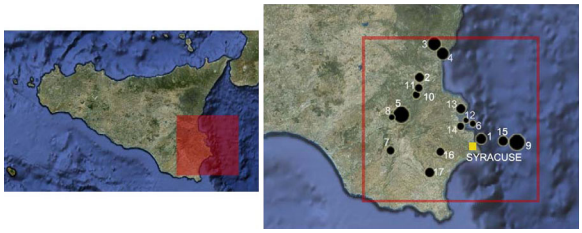

FIG. 2 (color online). Map of Sicily showing the location of the monitored site (yellow square) and epicenters (black circles) of nearby earthquakes (listed in Table I) that occurred during the monitoring period.

before large earthquakes [4,6]. In this case, AE bursts apparently indicate crustal stress crises affecting areas of a few hundred kilometers radius during the preparation of a seismic event. In spite of intrinsic difficulties in high-frequency propagation through disjointed media (in particular, at the ground-building foundation interface), part of the AE activity from the structures might derive from precursive microseismic activity. A rigorous investigation of causal relationships between AE bursts and earthquakes would require simultaneous operation of suitable arrays of AE monitoring sites, adequately placed in the territory, e.g., on the order of ~1000 over a large regional area.

Several studies established that the total rate of damage, as measured, for instance, by the accumulated AE released energy, increases as a power law of the time to failure on the approach to the structural collapse [7,8]. Here, the absence of a critical power-law behavior in the accumulated number of AE events in time, with two episodic abrupt increments at about 1800 and 2900 h (see Fig. 1), suggests that the structure experiences damage but is still far from unstable conditions.

Scaling law for AE and earthquake waiting-time distributions.—Space-time organization of AE and the earthquake source process is ruled by different power laws, among them, the Gutenberg-Richter law for the magnitude distribution [9], the Omori law for the rate of aftershocks as a function of time from the main shock [10], and the fractal distribution law for the epicenters [11]. However, power laws and critical exponents are not the only scaling predictions for fracture processes. Starting from the pioneer work of Bak *et al.* [12], Corral found that the distributions of waiting times between consecutive earthquakes follow a universal scaling law in different regions of the world and earthquake catalogs if appropriately rescaled [13]. There has been an ongoing debate in the seismological community about the extent to which universal scaling of earthquake temporal occurrence applies to AE time series in laboratory fracture [14–18]. This suggests that timing of fractures might be self-similar over a larger range of magnitude than had been suggested earlier. Here, the rescaling and collapsing procedure for waiting-time distributions in a sequence of rupture events is illustrated. We select the $N(M_{\text{th}})$ events with magnitude M above a certain threshold M_{th}. The sequence is transformed into a point process where events occur at times t_i with $1 \leq i \leq N(M_{\text{th}}) \equiv N$, and therefore, the waiting time between consecutive events can be obtained as $\tau_i \equiv t_i - t_{i-1}$. Thus, we compute the waiting-time probability density function (PDF) as $p_{M_{\text{th}}}(\tau) \equiv \text{Prob}(\tau \leq \text{waiting time} < \tau + d\tau)/d\tau$. Measuring the time in units of the mean waiting time $\langle\tau\rangle_{M_{\text{th}}} \equiv (t_N - t_1)/(N-1)$, i.e., performing the transformation $\tau \to \tau/\langle\tau\rangle_{M_{\text{th}}}$, changes also the units of the PDF: $p_{M_{\text{th}}}(\tau) \to \langle\tau\rangle_{M_{\text{th}}} p_{M_{\text{th}}}(\tau)$. This rescaling procedure is applied to PDFs obtained for

TABLE I. List of earthquakes with hypocentral distance from Syracuse ≤ 60 km (extracted from the Eastern Sicily earthquake catalog [5]). Richter magnitude, M_L; H, hypocenter depth; d, distance of monitoring site to the hypocenter; N_{AE}, AE rate.

	Date	Time	Epicentral coordinates		H (km)	d (km)	M_L
1	2006/09/19	03:20	37.09	15.35	20.2	21.4	2.0
2	2006/09/22	15:52	37.37	14.95	4.1	42.9	1.8
3	2006/09/26	16:59	37.62	15.14	13.6	62.0	2.5
4	2006/09/26	17:08	37.65	15.13	16.0	66.5	2.3
5	2006/10/14	23:55	37.25	14.78	18.4	50.8	3.0
6	2006/10/16	02:21	37.14	15.25	17.9	19.1	1.3
7	2006/10/16	03:40	37.05	14.76	16.7	48.5	1.6
8	2006/11/05	22:01	37.25	14.77	18.3	51.5	1.3
9	2006/12/05	05:01	37.06	15.61	24.3	38.8	2.9
10	2006/12/05	15:31	37.31	14.94	9.9	39.7	1.5
11	2006/12/07	16:23	37.34	14.93	0.0	40.9	1.6
12	2006/12/23	00:33	37.15	15.23	18.1	20.1	1.2
13	2006/12/25	08:02	37.23	15.17	16.1	24.6	1.8
14	2006/12/28	10:56	37.14	15.17	9.5	14.4	1.5
15	2007/01/09	09:57	37.08	15.57	14.0	30.1	1.9
16	2007/01/11	05:15	37.03	15.09	20.2	26.6	1.6
17	2007/01/14	23:23	36.90	14.98	17.6	37.2	1.9

several values of $M_{\rm th}$. If all the rescaled PDFs collapse onto a single curve f, we can establish the fulfilment of a scaling law [13]:

$$p_{M_{\rm th}}(\tau) = f(\tau/\langle\tau\rangle_{M_{\rm th}})/\langle\tau\rangle_{M_{\rm th}}. \quad (1)$$

The mean waiting time can be expressed in terms of the Gutenberg-Richter law [13,15]:

$$\langle\tau\rangle_{M_{\rm th}} = T10^{-a+bM_{\rm th}}, \quad (2)$$

where $T \equiv (t_N - t_1)$.

By inserting Eq. (2), Eq. (1) takes the form

$$p_{M_{\rm th}}(\tau) = 10^{-bM_{\rm th}}\tilde{f}(10^{-bM_{\rm th}}\tau), \quad (3)$$

where $\tilde{f}(10^{-bM_{\rm th}}\tau) \equiv kf(k10^{-bM_{\rm th}}\tau)$ and $k \equiv T^{-1}10^{a}$.

If we consider events separated by waiting times τ for $M \geq M_{\rm th}$ and $\tau' \equiv 10^{b}\tau$ for $M \geq M'_{\rm th} \equiv M_{\rm th} + 1$ and insert these particular arguments, $(\tau'; M'_{\rm th})$ and $(\tau; M_{\rm th})$, into Eq. (3), we obtain

$$p_{M_{\rm th}}(\tau) = 10^{b}p_{M_{\rm th+1}}(10^{b}\tau). \quad (4)$$

Equation (4) expresses self-similarity of the distributions, as they can be obtained from each other by a similarity transformation [15]. The scaling function f is well approximated by a generalized gamma distribution, which is a common parameterization for all fracture systems from the microscopic scale (AEs) to the seismic scale (earthquakes) [13–16]:

$$f(\theta) \propto \theta^{-(1-\gamma)}\exp[(-\theta/x)^{n}], \quad (5)$$

where θ is the rescaled waiting time: $\theta \equiv \tau/\langle\tau\rangle_{M_{\rm th}}$.

Although the parameterization of Eq. (5) is valid for all fracture processes, from AE in laboratory experiments to earthquakes, the values of fitting parameters γ, x, and n generally depend on the window of observation [13]. In particular, the power-law exponent $1-\gamma$ indicates the clustering degree in time of events. For example, when aftershock sequences or earthquake swarms dominate the selected time window T, the power-law exponent is high ($1-\gamma = 1.5$ [18] against 0.3 for stationary activity or slowly varying event rates [13–16]), indicating that earthquakes are close in time.

Previously, Kagan [19–21] in a different approach pointed out that the number of short waiting times between large earthquakes exceeds the number expected for memoryless Poisson recurrence. This behavior, indicating clustering, is the opposite of the regularity or quasiperiodicity derived from the idea of the seismic cycle. A surprising consequence of clustering is the paradoxical result that the longer it has been since the last earthquake, the longer the expected time until the next [13,19–21]. Here, below, the temporal occurrence of rupture events at different size scales will be investigated. First, we analyze the fracture process of a Syracuse limestone cylindrical specimen (base diameter 120 mm and height 120 mm). The specimen was subjected to uniaxial compression at a constant displacement rate of 0.1 μm s^{-1}, by using a servo-hydraulic press with a maximum capacity of 500 kN. We set the AE detection threshold to filter out background noise. In this way, we ensured that no spurious AE signals would be detected before the beginning of the test.

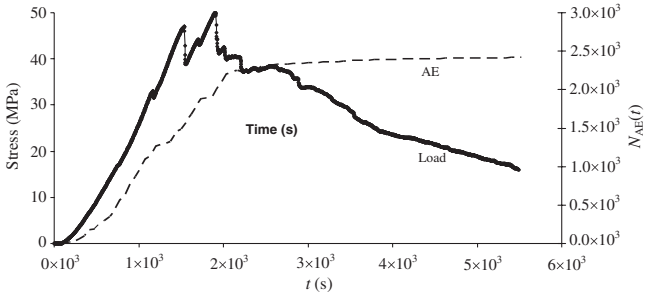

FIG. 3. Applied load (solid line) and accumulated number of AE events (dashed line) as functions of time.

In Fig. 3, the solid line represents the stress vs time diagram, characterized by irregular trend and stress drops due to damage accumulation before the specimen failure. Such quasibrittle behavior characterize heterogeneous materials [22]. The dashed line represents the accumulated number of AE events as a function of time. Stress drops were followed by as many drops in the AE activity, suggesting momentary relaxation until the stress exceeds the previous reached values (Kaiser effect [23]).

We analyze the AE time series until the peak stress, when the specimen fails, and also for the complete duration of the experiment. The PDFs of waiting times are calculated from both sequences and the corresponding rescaled distributions that appear in Fig. 4. In both cases, the data collapse illustrates the validity of a scaling law of the type of (5), although the scaling function f is different. The fit yields $\gamma = 0.23 \pm 0.02$, $x = 2.23 \pm 1.00$, and $n = 1.15 \pm 0.16$ before peak load and $\gamma = 0.46 \pm 0.04$, $x = 5.61 \pm 3.15$, and $n = 0.99 \pm 0.14$ for the whole duration of experiment. In the first case, the power-law exponent is

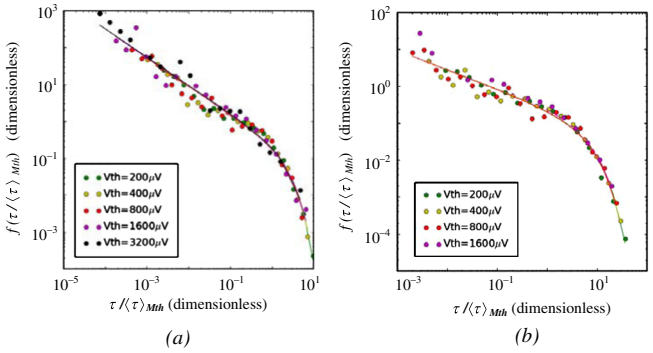

FIG. 4 (color online). Rescaled waiting-time PDFs for the period preceding the peak load (a) and for the whole duration test (b), for several $V_{\rm th}$ values, equivalent to $M_{\rm th} = \log(V_{\rm th}/1\ \mu{\rm V})$. The data collapse illustrates the fulfilment of a scaling law, where the solid line is the scaling function of Eq. (5).

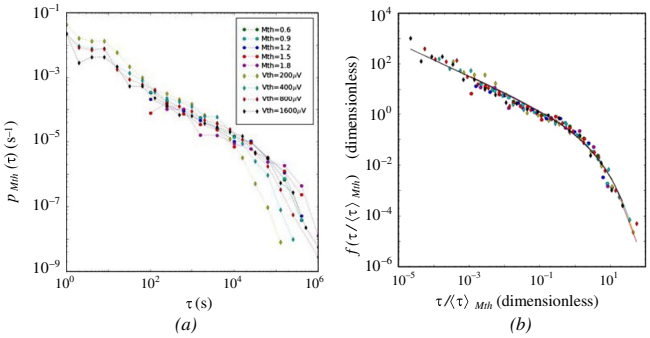

FIG. 5 (color online). Waiting-time PDFs for five seismic magnitude thresholds M_{th} and four AE signal thresholds V_{th} (a) and their collapse onto a single curve illustrating the fulfilment of a common scaling law (b).

higher ($1 - \gamma \approx 0.77$ against 0.54) because of the large number of AE events close in time which typically precede the specimen failure.

Now, we use the scaling approach to study the AE events from the pillar and the Eastern Sicily earthquakes. The PDFs of rescaled waiting times are calculated for both time series and appear in Fig. 5. The good quality of the data collapse demonstrates that a common scaling law describes both AE and earthquake time recurrence (the fit yields $\gamma = 0.35 \pm 0.02$, $x = 1.15 \pm 0.42$, and $n = 0.53 \pm 0.04$). This finding indicates the existence of a nontrivial correlation between small-scale AE activity in the temple pillar and nearby earthquake activity.

Conclusions.—An apparent correlation in time between AE bursts and the occurrence of nearby earthquakes is found. Therefore, the structure of the temple might be particularly sensitive to the action of nearby earthquakes. The demonstration that a common scaling law describes temporal recurrence of AE and earthquake activities supports the conjecture that both respond to critical values of stress in the same manner. The presented study suggests that the AE structural monitoring coupled with the analysis of local earthquake activity can be a tool of crucial importance in earthquake damage mitigation. The similarity between microfractures and seismicity could even have implications for understanding the triggering mechanism of earthquakes of all types by other earthquakes.

[1] C. H. Scholz, J. Geophys. Res. **73**, 1417 (1968).
[2] D. Lockner, Int. J. Rock Mech. Min. Sci. Geomech. Abstr. **30**, 883 (1993).
[3] S. Colombo, I. G. Main, and M. C. Forde, J. Mater. Civil Eng. **15**, 280 (2003).
[4] A. Carpinteri, G. Lacidogna, and G. Niccolini, Nat. Hazards Earth Syst. Sci. **7**, 251 (2007).
[5] Available at http://www.ct.ingv.it/ufs/analisti/gridsismMysql.asp.
[6] G. P. Gregori, G. Paparo, M. Poscolieri, and A. Zanini, Nat. Hazards Earth Syst. Sci. **5**, 777 (2005).
[7] A. Guarino, A. Garcimartin, S. Ciliberto, M. Zei, and R. Scorretti, Eur. Phys. J. B **26**, 141 (2002).
[8] D. L. Turcotte, W. I. Newman, and R. Shcherbakov, Geophys. J. Int. **152**, 718 (2003).
[9] C. F. Richter, *Elementary Seismology* (Freeman, San Francisco, 1958).
[10] T. Utsu, Y. Ogata, and S. Matsu'ura, J. Phys. Earth **43**, 1 (1995).
[11] J. Weiss, Surv. Geophys. **24**, 185 (2003).
[12] P. Bak, K. Christensen K, L. Danon, and T. Scanlon, Phys. Rev. Lett. **88**, 178501 (2002).
[13] A. Corral, in *Modelling Critical and Catastrophic Phenomena in Geoscience*, edited by P. Bhattacharyya and B. K. Chakrabarti, Lect. Notes Phys. Vol. 705 (Springer, Berlin, 2006), p. 191.
[14] J. Davidsen, S. Stanchits, and G. Dresen, Phys. Rev. Lett. **98**, 125502 (2007).
[15] G. Niccolini, F. Bosia, A. Carpinteri, G. Lacidogna, A. Manuello, and N. Pugno, Phys. Rev. E **80**, 026101 (2009).
[16] G. Niccolini, A. Schiavi, P. Tarizzo, A. Carpinteri, G. Lacidogna, and A. Manuello, Phys. Rev. E **82**, 046115 (2010).
[17] P. Diodati, F. Marchesoni, and S. Piazza, Phys. Rev. Lett. **67**, 2239 (1991).
[18] S. Hainzl, J. Geophys. Res. **107**, 2338 (2002).
[19] Y. Y. Kagan and D. D. Jackson, Bull. Seismol. Soc. Am. **89**, 1147 (1999).
[20] Y. Y. Kagan, Physica (Amsterdam) **77D**, 160 (1994).
[21] Y. Y. Kagan, in *Modelling Critical and Catastrophic Phenomena in Geoscience*, edited by P. Bhattacharyya and B. K. Chakrabarti, Lect. Notes Phys. Vol. 705 (Springer, Berlin, 2006), p. 303.
[22] D. Krajcinovic, *Damage Mechanics* (Elsevier, Amsterdam, 1996).
[23] J. Kaiser, Dr.-Ing. dissertation, Fakultät für Maschinenwesen und Elektrotechnik der Technischen Universität München (TUM), 1950.